biomass

MDPI

Article

Monitoring the Transformation of Organic Matter During Composting Using ^{1}H NMR Spectroscopy and Chemometric Analysis

Rubén Gonsálvez-Álvarez [1], Encarnación Martínez-Sabater [2], María Ángeles Bustamante [2], Mario Piccioli [3], José A. Saez-Tovar [2], Luciano Orden [2], Concepción Paredes [2], Raúl Moral [2] and Frutos C. Marhuenda-Egea [1,*]

[1] Department of Biochemistry and Molecular Biology and Agricultural Chemistry and Edafology, University of Alicante, Carretera San Vicente del Raspeig s/n, 03690 Alicante, Alicante, Spain; ruben.gonsalvez1@gmail.com
[2] GIAAMA Research Group, Centro de Investigación e Innovación Agroalimentaria y Agroambiental (CIAGRO-UMH), Agrochemistry and Environment Department, Miguel Hernández University, 03312 Orihuela, Alicante, Spain; e.martinezs@umh.es (E.M.-S.); marian.bustamante@umh.es (M.Á.B.); jose.saezt@umh.es (J.A.S.-T.); l.orden@umh.es (L.O.); c.paredes@umh.es (C.P.); raul.moral@umh.es (R.M.)
[3] Magnetic Resonance Center CERM, University of Florence, Via Luigi Sacconi 6, 50019 Sesto Fiorentino, Florence, Italy; piccioli@cerm.unifi.it
* Correspondence: frutos@ua.es

Abstract

Composting is an effective biotechnological process for transforming agro-industrial residues into stabilized and nutrient-rich organic amendments. However, the molecular mechanisms underlying organic matter transformation remain poorly resolved. In this study, a mixture of winery by-products and poultry manure was composted under controlled aeration and monitored through high-field ^{1}H NMR spectroscopy of the water-extractable organic matter (WEOM), followed by interval-based chemometric analysis. The NMR spectra revealed distinct compositional trends, including the rapid depletion of amino acids and carbohydrates, the transient accumulation of low-molecular-weight organic acids, and the gradual enrichment in aromatic and phenolic compounds associated with humification processes. Chemometric modeling using Partial Least Squares (PLS) regression and its interval variants (iPLS and biPLS) enabled accurate prediction of composting time ($r \approx 0.95$) and identification of diagnostic spectral intervals corresponding to key metabolites. These findings demonstrate the capability of NMR-based molecular profiling, combined with multivariate modeling, to elucidate the biochemical pathways of composting and to provide quantitative indicators of compost stability and maturity.

Keywords: co-composting; winery by-products; poultry manure; water-extractable organic matter (WEOM); ^{1}H NMR chemometrics

check for updates

Academic Editor: Bin Gao

Received: 9 October 2025
Revised: 12 November 2025
Accepted: 25 November 2025
Published: 1 December 2025

Citation: Gonsálvez-Álvarez, R.; Martínez-Sabater, E.; Bustamante, M.Á.; Piccioli, M.; Saez-Tovar, J.A.; Orden, L.; Paredes, C.; Moral, R.; Marhuenda-Egea, F.C. Monitoring the Transformation of Organic Matter During Composting Using ^{1}H NMR Spectroscopy and Chemometric Analysis. *Biomass* **2025**, *5*, 76. https://doi.org/10.3390/biomass5040076

Copyright: © 2025 by the authors. Licensee MDPI, Basel, Switzerland. This article is an open access article distributed under the terms and conditions of the Creative Commons Attribution (CC BY) license (https://creativecommons.org/licenses/by/4.0/).

1. Introduction

The massive generation of organic waste remains one of the primary environmental challenges for the sustainability of the agri-food sector in Europe. According to recent estimates, the European Union produces more than 220 million tons of agro-industrial residues annually, including by-products from the wine, livestock, and food industries [1]. These residues, rich in biodegradable organic matter, represent a potential resource for producing soil amendments that can improve soil quality and nutrient cycling in agricultural systems.

However, their inadequate management can lead to adverse environmental consequences, such as greenhouse gas emissions, leaching of pollutants, or the proliferation of pathogens.

Among the available treatment alternatives, composting has emerged as a cost-effective and biologically efficient technique to stabilize and valorize organic residues, resulting in a safe and nutrient-rich product suitable for agricultural application [2,3]. Composting reduces waste volume by approximately 50% and preserves essential macronutrients such as carbon, nitrogen, and phosphorus. The process is driven by the metabolic activity of complex microbial communities under controlled conditions of temperature, aeration, and moisture [4–6].

During composting, heat generation results from the microbial oxidation of organic substrates, leading to a self-heating process that can reach thermophilic temperatures. However, temperature, aeration, and moisture are externally regulated to maintain optimal conditions for microbial activity and hygienization [4–6]. In our composting setup, thermophilic exposure was ensured under the Rutgers static aeration regime, where 55 °C acts as the control setpoint that triggers continuous ventilation rather than a maximum temperature cap [7]. For the same mixture and operational conditions, previous studies reported effective pathogen reduction and compost hygienization as the process progressed, consistent with sustained thermophilic conditions and extended residence time [7,8]. Moreover, the long bio-oxidative phase and subsequent maturation under forced aeration are associated with the decline in phytotoxic intermediates and the attainment of compost stability and maturity [9].

Composting evolves through four successive microbiological and thermodynamic phases: initial mesophilic, thermophilic, cooling, and maturation [10,11]. In the mesophilic phase (20–40 °C), mesophilic bacteria and fungi degrade simple and readily available substrates such as carbohydrates, amino acids, and organic acids. The intense microbial activity generates heat, triggering the transition to the thermophilic phase. The subsequent thermophilic phase begins when temperatures exceed 45 °C and is dominated by thermophilic bacteria, actinomycetes, and fungi capable of degrading more complex polymers, including cellulose, hemicellulose, lipids, and proteins. This phase is essential for the hygienization of the compost [7], effectively eliminating pathogens and weed seeds. However, when temperatures surpass 65–70 °C, microbial activity and oxygen solubility may decline, potentially limiting the process [1]. As the process stabilizes, the cooling phase begins, enabling the recolonization by mesophilic organisms, notably actinomycetes and fungi that participate in the breakdown of recalcitrant compounds such as lignin. This culminates in the maturation phase, characterized by the formation of humic substances and the chemical stabilization of organic matter. The humification process is vital for producing high-quality compost with agronomic benefits, including enhanced soil structure, water retention, and nutrient availability [12].

The treatment of organic residues before agricultural application is essential to prevent the release of phytotoxic compounds and pathogens into soils and crops. Inadequate stabilization of agro-industrial or livestock wastes can lead to high concentrations of ammonia, volatile fatty acids, phenolic compounds, and heavy metals, which may impair plant growth and soil microbial activity. Composting ensures the hygienization and detoxification of these materials through controlled aerobic biodegradation, thereby reducing their environmental and health risks. Recent studies have documented the toxicity of improperly treated wastes and emphasized the benefits of compost stabilization before land application [8,13,14]. The final compost quality depends on several factors, including the initial C/N ratio, substrate composition, moisture content, and aeration. In particular, winery residues such as grape marc and animal manures like poultry litter contribute complex

mixtures of phenolic compounds, carbohydrates, proteins, and minerals that influence microbial succession and biochemical transformations [2,4].

A major challenge in composting is the objective assessment of compost maturity and stability. Immature compost may immobilize nutrients, release phytotoxic substances, and negatively impact crop performance. Several physical, chemical, and biological methods have been proposed to evaluate maturity, including C/N ratios, ammonium/nitrate content, respiration activity, and seed germination tests [15]. However, these approaches are often limited by variability in material composition and are not universally applicable.

Recently, spectroscopic techniques have emerged as powerful tools for compost analysis. Among them, proton nuclear magnetic resonance (^{1}H NMR) spectroscopy has proven effective in characterizing the soluble organic matter in compost, offering a non-destructive and highly informative approach [16,17]. Nuclear magnetic resonance (^{1}H NMR) spectroscopy of water-extractable organic matter (WEOM) provides a non-targeted window onto soluble metabolites that govern microbial activity and transformation pathways during composting. It allows the detection of amino acids, sugars, organic acids, alcohols, phenolics, and other compounds in soluble organic matter. Its holistic nature enables simultaneous monitoring of multiple metabolites without the need for separation procedures [16,18].

The use of high-field liquid-state nuclear magnetic resonance (NMR) spectroscopy at 900 MHz, combined with D_2O as solvent, provides a highly reliable analytical basis for interpreting these results. Unlike chromatographic methods, which may suffer from co-elution issues or matrix effects, NMR allows for unequivocal identification and quantification of organic compounds based on its distinct proton signals. This minimizes the risk of analytical artifacts and supports the conclusion that the observed fluctuations reflect real biogeochemical processes rather than methodological inconsistencies [7].

Here, we integrate ^{1}H NMR of WEOM with interval partial least squares (iPLS) and backward interval PLS (biPLS) to predict composting time and to localize informative spectral domains [19,20]. Complementing these models, we implement a bin-wise correlation screen that combines Pearson and Spearman coefficients with power and exponential fits, thereby prioritizing signals that evolve monotonically (linearly or non-linearly) with process time. This dual strategy is applied to a co-composting mixture of winery residues and poultry manure, enabling both mechanistic interpretation (e.g., VFAs (volatile fatty acids), amino acids, tartrate, glycerol, dicarboxylic acids such as suberate) and compact marker discovery. The present study aims to: (i) map the molecular trajectory of WEOM across composting stages; (ii) develop and validate interval-based PLS models for time prediction; and (iii) identify high-confidence NMR markers that correlate strongly with composting time and align with biochemically interpretable pathways. By combining full-spectrum fingerprints with focused statistics, we demonstrate a practical framework that captures both fast-degrading labile fractions and longer-term humification trends, offering actionable maturity indicators beyond conventional metrics [2,10–12]. The approach is general and can be ported to other residue blends, while targeted 2D-NMR/MS validation of tentative assignments remains a priority for broader deployment.

2. Materials and Methods

2.1. Composting Substrate and Pile Composition

The composting experiment was carried out using a mixture of agro-industrial residues composed of de-exhausted grape marc (EGM) (70%, as percentage on a fresh weight basis) and poultry manure (PM) (30%, as percentage on a fresh weight basis). These materials were selected due to their high content of biodegradable organic matter and their prevalence in agricultural waste streams. PM was collected from a poultry farm with

30,000–40,000 laying hens located in Orihuela (Alicante, Spain), and EGM from an alcohol distillery placed in Villarrobledo (Albacete, Spain).

Before forming the composting pile, representative samples of each component were collected using a stratified random sampling method. Specifically, seven subsamples were taken from different points along the vertical and horizontal profile of the materials, and then homogenized to obtain a composite sample. The pile was constructed outdoors and monitored throughout the composting process. The sampling protocol followed the European Union Directive 77/535/CEE, amended by 87/566/CEE, for fertilizers under 2.5 tonnes in mass [2].

The mixtures (about 1800 kg each) were composted in a pilot plant, in trapezoidal piles (1.5 m high with a 2 × 3 m base). The Rutgers static pile composting system was used [21], being the air supplied by forced aeration conducted through three basal PVC tubes (3 m length and 12 cm diameter). The aeration system imposed was 30 s every 30 min, with 55 °C as the ceiling temperature for continuous ventilation. In this context, 55 °C denotes the operational threshold that activates continuous ventilation in the Rutgers system rather than a hard upper temperature limit; the pile remained in sustained thermophilic conditions throughout the bio-oxidative phase. The process lasted 212 days, during which three main phases were observed: mesophilic (0–14 d), thermophilic (15–157 d), and maturation (158–212 d). Temperature was recorded daily at three depths, reaching peaks of about 50 °C during the thermophilic stage. Forced aeration was maintained throughout the bio-oxidative phase (157 d) and then stopped for maturation. Moisture content was monitored weekly and maintained above 40% by periodic watering, with leachate being collected and reintroduced into the pile. A single pilot-scale pile was used for this experiment to maintain homogeneous conditions throughout the composting process [7,9].

2.2. Composting Process, Sampling, and Extraction of Soluble Organic Matter

The composting pile was monitored for a period of several weeks, during which temperature profiles were recorded to characterize the mesophilic, thermophilic, and maturation phases. Samples were taken at predetermined time points, covering all composting stages from initial mixing to final stabilization. At each sampling event, seven subsamples were collected from different pile zones (upper, central, and basal layers) and at various depths to capture spatial variability. The subsamples were thoroughly mixed to produce a composite sample. The composite sample was air-dried and ground to 0.5 mm to obtain aliquots for water extraction and NMR analysis. This procedure ensured that each sample represented the average composition of the entire composting mass at the corresponding time point.

To analyze the water-soluble fraction of organic matter, 1 g of fresh compost was mixed with 20 mL of distilled water containing 1 mM sodium azide to prevent microbial activity during extraction. The mixture was stirred for 16 h at room temperature.

After extraction, the samples were decanted and centrifuged at 15,000 rpm for 15 min at 4 °C. The supernatant was stored at −20 °C until further analysis.

2.3. ^{1}H NMR Spectroscopy

^{1}H NMR, TOCSY, HSQC and HMBC spectra of the extracted soluble organic matter were acquired using a Bruker 900 MHz UltraShield NMR spectrometer (Bruker, Rheinstetten, Germany), equipped with a 5 mm inverse probe. For each sample, 550 µL of the aqueous extract was mixed with 50 µL of deuterium oxide (D_2O) as a field lock solvent. A pre-saturation sequence was applied to suppress the water peak. Spectra were recorded at room temperature. All spectral data were processed using TopSpin 4.0.6 (Bruker, Rheinstetten, Germany), including Fourier transformation, phase and baseline correction.

The spectral region of interest (0.5 to 9.5 ppm) was divided into integral segments of 0.02 ppm for statistical analysis, following standard protocols for metabolomic studies on complex mixtures [16,19].

2.4. Chemometric Analysis

Chemometric analysis was performed using MATLAB R2008b. Multivariate regression methods, specifically interval Partial Least Squares (iPLS) and backward interval Partial Least Squares (biPLS), were applied to identify informative spectral regions associated with compost maturity stages (iToolbox). Model validation was performed using cross-validation, and performance was evaluated based on the root mean squared error of cross-validation (RMSECV) and correlation coefficients (r) between predicted and observed values. These methods allowed for the interpretation of dynamic changes in the composition of soluble organic matter and the identification of NMR signal regions most relevant to composting progression. MATLAB version 2024 (MathWorks, Natick, MA, USA) is used for the calculations, and the iToolbox is available at https://ucphchemometrics.com/186-2/algorithms/ (accessed on 9 October 2025)

To identify ^{1}H NMR regions that co-vary with composting time, we applied a bin-wise correlation screen using the aligned, baseline-corrected spectra binned at 0.02 ppm (full spectral width). For each bin, we analyse (i) the Pearson correlation coefficient (r) as a sensitive detector of linear trends; (ii) the Spearman rank correlation (ρ) to capture monotonic but non-linear relationships robust to outliers; and (iii) the distance correlation (dCor), which detects arbitrary dependence structures beyond monotonicity. In parallel, we fit parametric non-linear models that are chemically plausible for first-order formation/decay—power and exponential functions—recording their R^2 as an effect-size measure. The algorithm standardizes and aggregates these metrics into a consensus rank so that bins prioritized as "top hits" show agreement across linear, rank-based, and model-based criteria. Final candidates were visually inspected to confirm a coherent time trajectory, stable local baseline, and absence of artifactual alignment edges, and were cross-checked against chemically interpretable assignments and the informative intervals revealed by iPLS/biPLS. This multi-criteria, rank-aggregation approach reduces false positives driven by any single metric and favors peaks with both statistical strength and biochemical plausibility.

3. Results

3.1. General Spectral Characteristics of Soluble Organic Matter

^{1}H NMR spectra of the water-extracted compost samples revealed a complex mixture of organic compounds across all composting stages. The main signal regions corresponded to aliphatic protons (0.5–3.0 ppm), sugars and alcohols (3.0–6.0 ppm), and aromatic and phenolic compounds (6.0–9.0 ppm). These spectral zones are consistent with previous studies on compost and humified organic matter [16,18] (Figures 1 and 2). Compound identification in Table 1 was based on comparison with published ^{1}H NMR data for compost and soil organic extracts [6,16]. Additional verification was achieved by inspecting two-dimensional NMR spectra (COSY, TOCSY, HMBC and HSQC) and by cross-checking chemical-shift values and multiplicities against the Human Metabolome Database (HMDB), the Biological Magnetic Resonance Data Bank (BMRB), and the Chenomx NMR Suite 8.2 software (Chenomx Inc., Edmonton, AB, Canada).

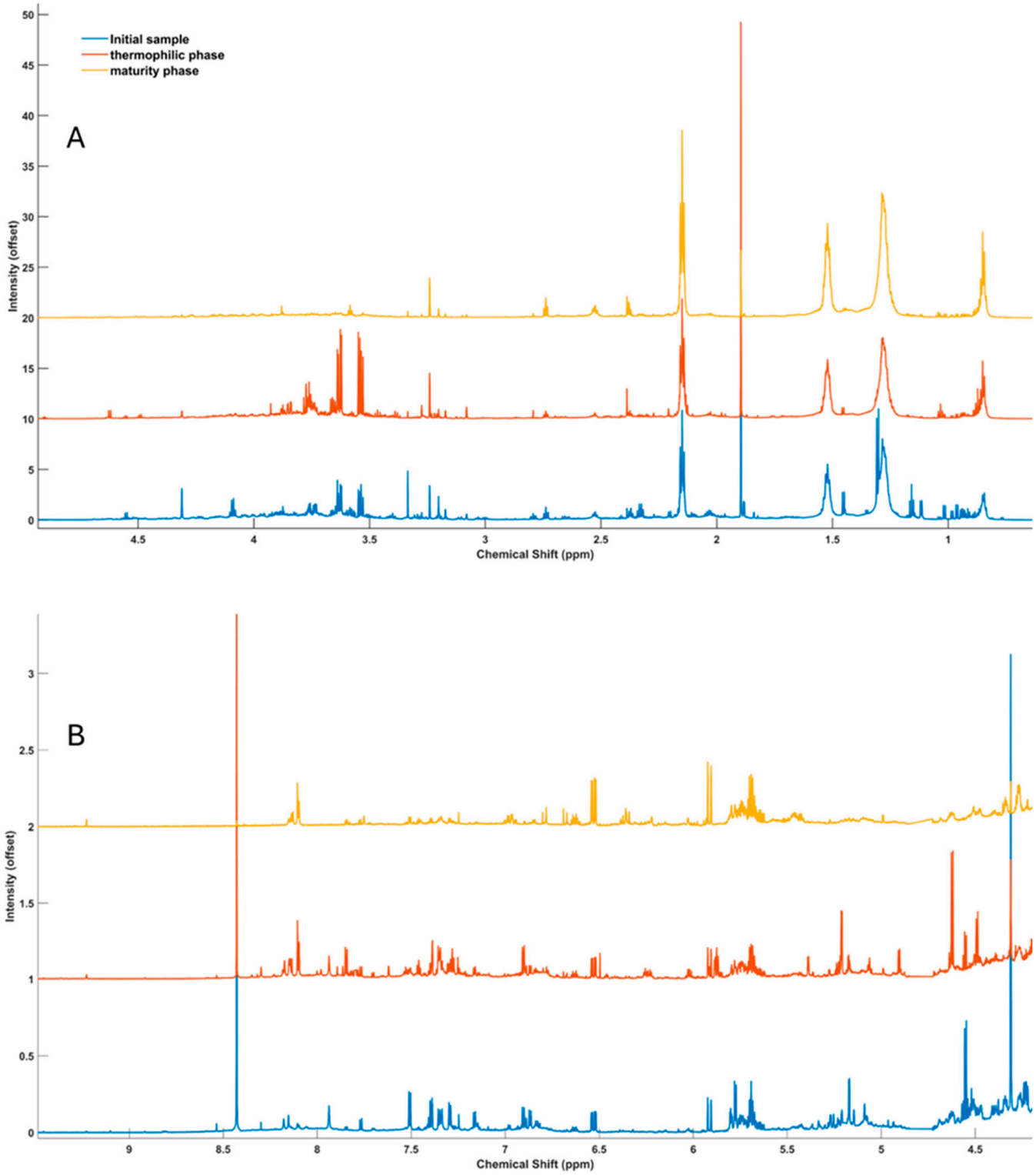


Figure 1. One-dimensional ^{1}H NMR spectra of water extracts at three composting stages. Representative spectra from the initial sample, a thermophilic-phase sample, and a maturation-phase sample are shown in two spectral windows: (**A**) 0.00–4.60 ppm (aliphatic region including organic acids, alcohols and carbohydrates) and (**B**) 5.00–10.00 ppm (olefinic/aromatic region).

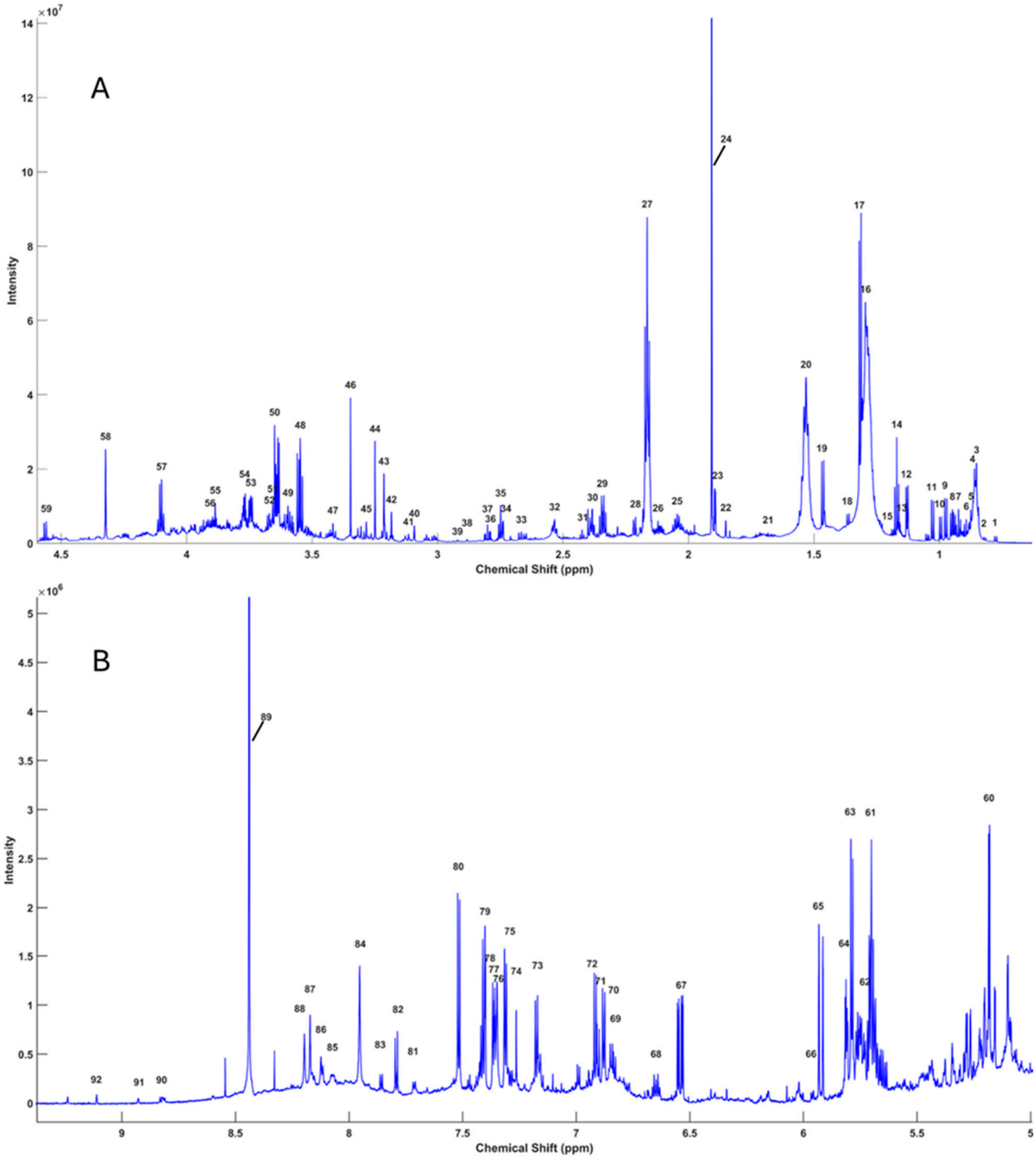


Figure 2. Annotated ^{1}H NMR spectrum of the initial sample (water extract). The spectrum is displayed in two windows: (**A**) corresponds to the section of the ^{1}H NMR spectrum between 0.6 and 4.6 ppm, and (**B**) corresponds to the section of the ^{1}H NMR spectrum between 5.0 and 9.8 ppm. Numbered peak labels referring to the assignments listed in Table 1 (compound name and multiplicity). This numbering is used consistently throughout the manuscript when referring to individual resonances.

Table 1. Assignment of ^{1}H NMR resonances in water extracts of compost samples. The table lists the peak number used in Figure 2, the chemical shift (δ, ppm), the compound name, and the multiplicity observed in the 1D spectrum.

Peak	δ (ppm)	Compound	Multiplicity
1	0.779	unassigned	d
2	0.823	2-Hydroxyvalerate	d
3	0.852	Caprate	t
4	0.859	Octenoate	t
5	0.874	Valerate	t
6	0.892	Isovalerate	t
7	0.923	Isoleucine	t
8	0.948	Leucine	t
9	0.978	Valine	d
10	0.998	Leucine	d
11	1.030	Valine	d
12	1.132	Proppylene glycol	d
13	1.164	Isopropanol	d
14	1.169	Ethanol	t
15	1.189	3-Hydroxybutirate	d
16	1.294	Suberate	m
17	1.319	Lactate	d
18	1.367	Acetoine	d
19	1.468	Alanine	d
20	1.531	Suberate	t
21	1.682	Leucine	m
22	1.851	Timidine	s
23	1.894	1-aminocyclopropane carboxilic acid	t
24	1.907	Acetate	s
25	2.045	Glutamate	m
26	2.121	Glutamate	m
27	2.164	Suberate	t
28	2.210	Levulinate	s
29	2.346	Glutamate	m
30	2.384	Levulinate	t
31	2.423	Oxoglutarate	t
32	2.533	Guanidine succinate	m
33	2.665	Aspartate	dd
34	2.738	Sarcosine	s
35	2.748	Levulinate	t
36	2.789	Aspartate	dd
37	2.800	Methyl guanidine	s
38	2.882	TMA	s

Table 1. *Cont.*

Peak	δ (ppm)	Compound	Multiplicity
39	2.920	N,N-Dimethylglicine	s
40	3.092	unassigned	s
41	3.115	Malonate	s
42	3.180	Choline	s
43	3.216	sn-glycerol-3-phosphocholine	s
44	3.242	TMAO	s
45	3.289	Xylose	t
46	3.346	Methanol	s
47	3.417	Propylene glycol	q
48	3.547	Glycerol	m
49	3.596	4-Hydroxybutirate	t
50	3.649	Glycerol	m
51	3.656	Ethylene glycol	s
52	3.670	Ethanol	q
53	3.744	Glutamate	m
54	3.766	Glycerol	m
55	3.886	Betaine	s
56	3.895	Aspartate	m
57	4.099	Lactate	q
58	4.322	Tartrate	s
59	4.559	Xylose	d
60	5.180	Xylose	d
61	5.701	unassigned	t
62	5.717	Cis-aconitate	s
63	5.791	Uracil	d
64	5.812	2-Octanoate	dt
65	5.931	Gibberelline	d
66	5.966	cis-cis-Muconate	dd
67	6.534	Gibberelline	dq
68	6.648	2-Octanoate	dt
69	6.827	2-Aminobenzoic	ddd
70	6.850	2-Aminobenzoic	dd
71	6.884	Tyrosine	d
72	6.927	4-Hydroxybenzoate	d
73	7.170	Tyrosine	d
74	7.264	Syringate	s
75	7.316	Phenylalanine	d
76	7.348	Thymine	s
77	7.358	2-Aminobenzoic	ddd

Table 1. *Cont.*

Peak	δ (ppm)	Compound	Multiplicity
78	7.368	Phenylalanine	t
79	7.401	Phenylalanine	d
80	7.521	Uracyl	d
81	7.718	2-Aminobenzoic	dd
82	7.787	4-Hydroxybenzoate	d
83	7.863	Benzoate	d
84	7.953	Xanthine	s
85	8.073	Trigonelline	m
86	8.123	unassigned	d
87	8.171	Hypoxantine	s
88	8.196	Hypoxantine	s
89	8.439	Formic acid	s
90	8.822	Trigonelline	m
91	8.927	Nicotinate	d
92	9.112	Trigonelline	s

Abbreviations: s, singlet; d, doublet; t, triplet; q, quartet; m, multiplet; dd, doublet of doublets; dt, doublet of triplets; dq, doublet of quartets.

^{1}H NMR spectra were recorded only for the composite mixture of de-alcoholized grape marc and poultry manure used in the composting process. The purpose of the present study was to monitor the molecular evolution of the system as an integrated whole rather than to characterize each raw material separately. The individual composition of these residues has been thoroughly described in previous studies [22].

The evolution of conventional maturity indicators (temperature, C/N ratio, pH, electrical conductivity, ammonium/nitrate ratio, and germination index) for this same composting pile has been fully described elsewhere [7,9]. Those studies demonstrated that the compost produced under the Rutgers forced-aeration system reached a stable and hygienized state, satisfying the maturity criteria required for agricultural use [7–9]. These data showed a typical evolution for a well-managed composting process, with pH rising from 6.2 to 8.3, electrical conductivity increasing from 3.5 to 6.8 dS m^{-1}, total organic carbon decreasing from 46 to 29% (dry weight), and a final C/N ratio of about 12.5, consistent with compost stability and maturity. These results validate the correct progression of the composting process under the same operational conditions described in the present study. Therefore, the present work focuses on the molecular evolution of the water-extractable organic matter (WEOM) through ^{1}H NMR and chemometric analysis as a complementary and more detailed characterization of the transformation process.

In the initial samples, signals corresponding to amino acids (e.g., alanine, valine, glutamic and aspartic acid), volatile fatty acids (e.g., acetic, lactic, valeric acids), and sugars (e.g., glucose, xylose) were clearly identifiable (Table 1 and Figure 2). This profile reflects the fresh, labile nature of the organic material at the start of composting, particularly given the high protein and carbohydrate content of poultry manure and grape marc.

^{1}H NMR spectra recorded over time showed a non-linear evolution of soluble organic matter (Figure 1). During the initial mesophilic phase, a marked decline was observed in the peaks corresponding to amino acids and sugars (Figure 1), consistent with microbial consumption of labile substrates. The increasing signals for organic acids during this period

were linked to intermediate fermentation products, contributing to a drop in pH within the compost mass [23].

In the thermophilic phase, elevated temperatures promoted the enzymatic degradation of structural polymers, particularly cellulose, hemicellulose, and proteins [23]. The decrease in signals related to polyalcohols and fermentative alcohols (e.g., ethanol, methanol) indicated both volatilization and biodegradation.

Of particular interest is the behavior of aromatic signals, which intensified during the mid-stages of composting, suggesting the partial depolymerization of lignin and the release of phenolic substructures (Figure 1). These changes were accompanied by enzymatic activity associated with cellulases, hemicellulases, and ligninolytic enzymes [24].

Once the peaks of the ^{1}H NMR spectrum have been identified, we can evaluate how these signals change during the composting process. We observe that many signals disappear due to the metabolism of microorganisms, while other signals undergo variations also associated with this highly varied metabolism. Other signals, associated with more recalcitrant compounds, such as medium- and short-chain organic acids, such as suberin (octanedioic acid), remain throughout the composting process. The presence of different biomolecules is determined by the initial materials used in the compost pile. For example, the presence of ethanol or tartaric acid (Table 1) indicates that materials from the wine industry have been used.

A few minor resonances (e.g., δ = 0.779 ppm and 3.092 ppm) remained unassigned even after analysis of complementary 2D NMR spectra (TOCSY, HSQC, HMBC). These peaks likely correspond to low-abundance or overlapping metabolites. The aliphatic resonance near 0.78 ppm may arise from branched short-chain fatty acids such as isobutyrate or isovalerate, whereas the singlet at 3.09 ppm could reflect methylene groups adjacent to carbonyl or quaternary amine centers, as in malonate or N,N-dimethylglycine [25–27]. Confirmation of these tentative assignments will require targeted LC–MS/MS analysis in future work.

The aqueous extracts obtained during composting of the winery by-products and poultry manure mixture displayed a complex array of low-molecular-weight organic compounds that evolved markedly over the course of the process. Among the most abundant solutes, acetate dominated the spectra (ca. 285‰, 1.91 ppm), consistent with the accumulation of volatile fatty acids (VFAs) during the early acidogenic stages of biodegradation. Such compounds are well documented in the decomposition of poultry manure and other organic feedstocks, where they appear transiently and decrease as the process stabilises [28,29]. In agreement with previous NMR-based characterisations of water-extractable organic matter (WEOM), these VFAs represent the hydrophilic and labile fraction that is consumed as composting progresses [30].

Lactate was also prominent in the spectra (≈60‰; 1.32 ppm). This metabolite is a hallmark of lactic fermentation and has been frequently observed during the early stages of organic matter transformation, where it is rapidly metabolised by secondary microbial communities. Formate, which accounted for ca. 49‰ at 8.44 ppm, was another significant component. Formate has been previously detected in water-extractable fractions of compost and is generally associated with microbial oxidation processes in early stages of degradation [30].

Signals corresponding to amino acids, such as valine, leucine, isoleucine, and glutamate, were clearly identified (each contributing between 7–9‰). Their relative intensity decreased rapidly with composting time, consistent with the recognised fast utilisation of free nitrogenous solutes by the microbial community. Similar patterns of amino acid depletion in the WEOM pool during composting have been reported in both ^{1}H- and ^{13}C-NMR studies [31,32].

The rapid attenuation of amino acid signals during the early composting phase reflects intense microbial proteolysis and amino acid catabolism. Extracellular proteases and peptidases hydrolyze complex proteins into free amino acids, which are then deaminated by transaminases and dehydrogenases such as glutamate dehydrogenase, alanine dehydrogenase, and aspartate dehydrogenase. These reactions release ammonium and produce keto-acids (e.g., pyruvate, α-ketoglutarate) that feed the tricarboxylic acid (TCA) cycle, supporting microbial energy metabolism and growth [33,34]. Thermophilic microorganisms, including *Bacillus*, *Thermobifida*, and *Actinomycetes,* are known to express thermostable proteolytic and deaminating enzymes that accelerate nitrogen turnover and account for the sharp decline in amino-acid resonances observed in the ^{1}H NMR spectra [35–38].

Polyalcohols were also detected, most notably glycerol (≈9.8‰; 3.77 ppm) and ethylene glycol (≈8.2‰; 3.66 ppm). The presence of glycerol is highly indicative of a winery origin, since this compound is a primary product of yeast fermentation and is well documented in grape marc, lees, and wines [39,40]. Its dynamics during composting likely reflect both release from residual yeast biomass and subsequent microbial consumption. Tartrate, another distinctive solute of vinicultural residues, was also detected; tartaric acid is the dominant organic acid in grape marc and winery wastes and is frequently reported in chemical characterisations of such by-products [41].

Several dicarboxylic acids were identified, including a suite of peaks corresponding to suberate (octanedioic acid), which together represented more than 110‰. Suberic acid may originate from ω-oxidation of fatty acids but is also a characteristic monomer of suberin, the major biopolymer of cork. Its occurrence in winery-related residues is therefore not unexpected. Moreover, migration of suberic acid from cork stoppers into wines has been previously demonstrated, providing further evidence for this source [42,43].

Aromatic resonances in the 6–8 ppm region became progressively more intense as composting advanced. This shift reflects the well-documented transition from labile O-alkyl structures, such as carbohydrates and small metabolites, towards more recalcitrant and aromatic moieties during humification. The enrichment of aromatic signals and the relative depletion of aliphatic ones are consistent with previous NMR studies that tracked compost maturation through increasing complexity of the WEOM fraction [30,31]. The gradual increase in the aromatic region (6–8 ppm) of the ^{1}H NMR spectra indicates a relative enrichment of aromatic and phenolic protons resulting from the preferential decomposition of aliphatic and O-alkyl compounds. Because all spectra were normalized by total integral area, this trend represents a structural shift rather than an absolute rise in total carbon. Independent determinations of total organic carbon (TOC) and C/N ratio for the same composting experiment [9] revealed progressive mineralization, consistent with the molecular evidence for humification. Although the absolute NMR changes were modest, fluorescence excitation–emission matrix (EEM) analyses of the same water extracts showed a clear increase in humic-like fluorescence, supporting the formation of conjugated aromatic structures [44–46]. Overall, the combined NMR–EEM evidence suggests a compositional transformation toward more recalcitrant organic matter, in line with previous studies of compost and soil humification [2,47].

Finally, transient signals attributable to methanol were also observed. In viticultural matrices, methanol derives from pectin demethylation and is a regulated constituent of wines [48]. Its disappearance during composting is most likely due to volatilisation and microbial degradation, processes that have been reported in analogous systems. Besides volatilization, the progressive attenuation of methanol signals likely reflects its involvement in microbial and enzymatic transformation pathways. Methylotrophic microorganisms—including species of *Methylobacterium*, *Hyphomicrobium*, and thermophilic *Bacillus*—oxidize

methanol through sequential reactions catalyzed by methanol dehydrogenase (MDH) and formaldehyde dehydrogenase, yielding formate and ultimately CO_2 [49,50].

In parallel, pectin methylesterases (PMEs) act on plant-derived polysaccharides, releasing methanol from methyl-esterified pectins [51]. A fraction of this methanol may subsequently participate in aromatic methylation reactions mediated by O-methyltransferases (OMTs), contributing to the formation of methoxylated phenolics [52]. These complementary microbial and enzymatic processes explain the transient presence of methanol detected by ^{1}H NMR and support its role as a reactive intermediate in the carbon-turnover network of composted organic matter [53].

In the aliphatic low-ppm window (0–5 ppm), several minor yet informative signals point to biochemical routes typical of wine-residue composting. A weak singlet attributable to choline would be consistent with anaerobic choline metabolism to trimethylamine (TMA) via the glycyl-radical enzyme CutC; this pathway is broadly distributed in environmental microbiomes and is well established biochemically [1–3]. The detection of levulinate/levulinic acid at trace levels is also notable, as levulinic acid is a recognized biomass-derived platform molecule formed from carbohydrate dehydration/hydrolysis cascades; its presence is chemically plausible in lignocellulosic matrices undergoing acidic/autohydrolytic microenvironments during composting [4–6]. In addition, a small resonance assignable to 3-hydroxybutyrate would be compatible with microbial turnover of bacterial polyhydroxyalkanoates (PHAs) such as PHB, for which enzymatic depolymerization to 3-hydroxybutyrate is documented and biodegradation under composting conditions is frequently observed [7–9].

Within the aromatic region (≈5–10 ppm), faint signals consistent with xylose-derived fragments (e.g., anomeric protons of pentoses) support xylan/hemicellulose deconstruction, a common fate of agricultural residues; xylan depolymerization liberates xylose and arabinose under the combined action of xylanases, arabinofuranosidases, and related accessory enzymes [10,11]. More specifically, syringic acid and p-hydroxybenzoic acid are credible minor constituents in grape-derived composts: both are repeatedly reported among the hydroxybenzoic acids of grape pomace, with syringic acid often abundant and linked to anthocyanin breakdown (malvidin-3-glucoside) [12–14]. Finally, very small aromatic resonances assignable to purine metabolites (xanthine/hypoxanthine) would be chemically coherent with the poultry manure fraction: these bases are detectable in poultry litter and evolve during storage/composting [15,16]. As an additional, matrix-specific marker, traces tentatively attributable to suberic acid are plausible given the cork fraction in winery residues; suberin-derived monomers, including suberic acid, can migrate from cork and have been measured in hydroalcoholic media and wines [17,18].

3.2. Chemometric Analysis of Composting Progress

^{1}H NMR spectra recorded over time showed a non-linear evolution of soluble organic matter. During the initial mesophilic phase, a marked decline was observed in peaks corresponding to amino acids and sugars (Figures 1 and 2), consistent with microbial consumption of labile substrates. The increasing signals for organic acids during this period were linked to intermediate fermentation products, contributing to a drop in pH within the compost mass.

In the thermophilic phase, elevated temperatures promoted the enzymatic degradation of structural polymers, particularly cellulose, hemicellulose, and proteins. The decrease in signals related to polyalcohols and fermentative alcohols (e.g., ethanol, methanol) indicated both volatilization and biodegradation.

To quantitatively evaluate the progression of composting, chemometric models were constructed using interval Partial Least Squares (iPLS) and backward interval PLS (biPLS)

(Figures 3 and 4). These results highlight the diagnostic power of NMR in detecting unexpected chemical features in compost feedstocks, which may influence the composting dynamics or raise safety concerns.

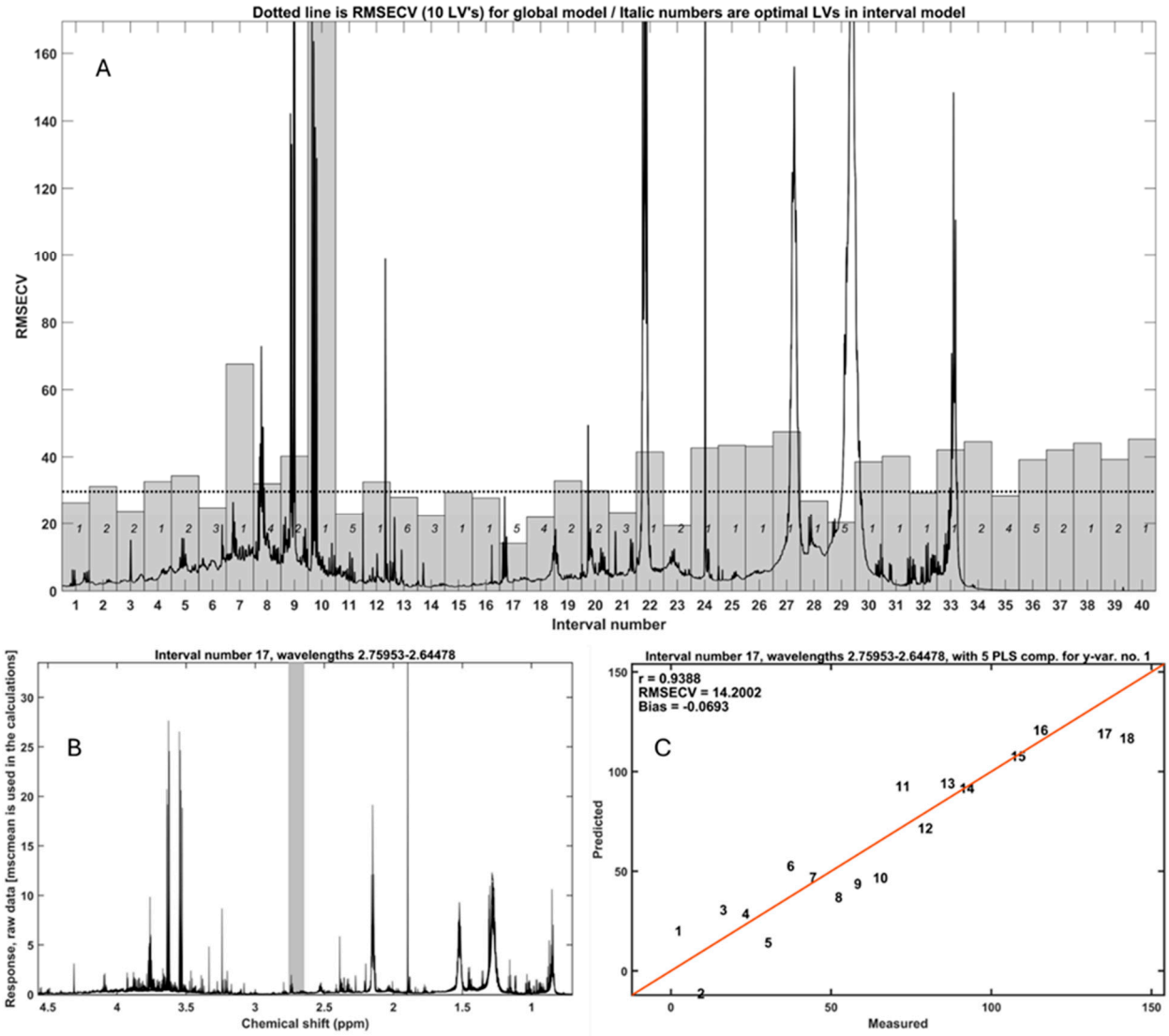


Figure 3. Interval Partial Least Squares (iPLS) modelling of composting time from ^{1}H NMR spectra. (**A**) Interval-performance map from the iPLS model built on the aligned spectra using 40 equal-width intervals. (**B**) Predicted-vs-measured plot for the best single-interval model (as identified in panel (**A**)), with the optimal number of latent variables. (**C**) Predicted-vs-measured plot for the best single-interval model with 5 LVs (latent variables).

In Figure 3, we can observe the presence of a triplet (2.74 ppm), which corresponds to the levulinate signals. However, we do not observe this signal to have a significant decay during the composting process. Minority signals are more difficult to assign and track their evolution during composting. To enhance interpretability and predictive performance, biPLS regression was applied, eliminating non-informative spectral intervals and focusing on regions highly correlated with composting. The final model, based on selected intervals in the amino acid (0.5–2.5 ppm) and carbohydrate (3.0–4.5 ppm) domains, achieved a strong correlation (r = 0.951) and low prediction error (RMSECV = 13.04) (Figure 4).

With biPLS, we have been able to identify four regions of the ^{1}H NMR spectrum that contain information allowing us to obtain a good correlation between these regions and composting time. One of the most important regions contains the peak around 1.23 ppm,

which corresponds to an organic acid such as succinic acid. The signal for levulinate (2.74 ppm) also appears, as do the signals associated with lactate, which appear both in the region where succinic acid appears (1.33 ppm) and in the region of 4.11 ppm. These chemometric methods can have problems with overfitting. In fact, when reviewing the results, we observe that there is no clear relationship between the signals identified in the regions with the best correlation with the composition time.

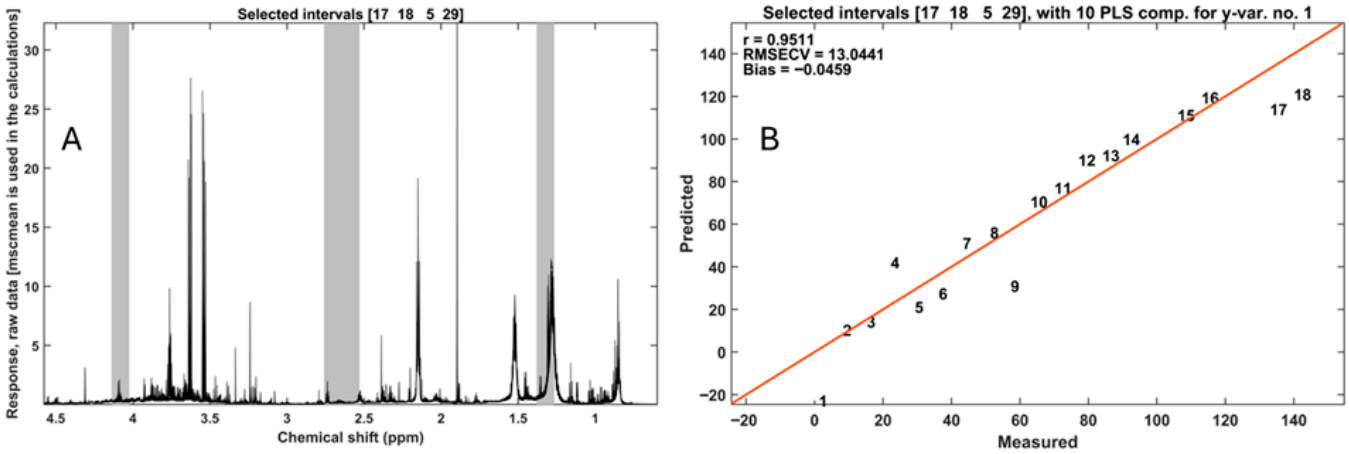


Figure 4. Backward interval PLS (biPLS): interval selection and final multi-interval model. (**A**) Interval-retention trajectory from the biPLS algorithm run on the aligned ^{1}H NMR spectra, highlighting the four informative regions retained at the optimum. (**B**) Predicted-versus-measured composting time for the final multi-interval model constructed with the retained intervals [17 18 5 29], yielding r = 0.951 and RMSECV = 13.04 days over a 212-day window (≈6.2% relative error).

The backward interval PLS (biPLS) regression model, implemented using the iToolbox for MATLAB [19,54], achieved a high correlation coefficient (r = 0.951) and a root mean square error of cross-validation (RMSECV) of 13.04 days with 5 LVs. In this context, "LVs" denotes latent variables, which are the components extracted by the PLS algorithm that represent the underlying covariance structure between the spectral matrix (X) and the response variable (Y). Given the total composting duration of 212 days, this RMSECV represents a relative prediction error of only 6.2%, which is well within the range of robust chemometric models for long-term biological processes [55,56]. The model successfully identified four key spectral intervals (1.27–1.38, 2.53–2.64, 2.64–2.76, and 4.02–4.13 ppm) as highly informative for tracking composting progression, confirming the utility of 1 H NMR as a quantitative tool for compost maturity assessment.

The iPLS and biPLS models were internally validated using a five-segment Venetian-blinds cross-validation strategy implemented in the iToolbox for MATLAB [19,54]. Although the limited number of samples did not allow an independent test set, this approach minimizes overfitting and provides reliable estimates of predictive accuracy for small datasets [57,58]. Future work will apply these models to independent composting runs and feedstock mixtures to evaluate external predictivity following best-practice guidelines [19].

The four spectral intervals retained by the biPLS model (1.27–1.38, 2.53–2.76, 4.02–4.13 ppm) correspond to chemically interpretable regions dominated by lactate and suberate (aliphatic domain), aspartate/levulinate (2.6–2.7 ppm), and tartrate (4.1 ppm). The temporal evolution of these metabolites mirrors the composting progression, providing mechanistic validation of the statistical selection and supporting the biochemical relevance of the predictive model [59].

To find a clearer correlation between the signals observed in the ^{1}H NMR spectra and the composting time, we have designed strategies that differ from the regression methods used previously. One of these strategies would be developed in different stages. The peaks

could be identified and then considered to be present in all spectra to see if they correlate with composting time. However, this strategy assumes that the same peaks will be present in all spectra over time. We opted for the strategy of dividing the spectrum into 0.02 ppm regions and integrating the signal in those intervals. This is called binning.

Once the integrals corresponding to each interval have been calculated, we will have to evaluate other types of correlations different from the linear correlation used by iPLS and bi-PLS. We look for correlations between binned integrals and the composting time at which the different samples were obtained (Figure 5).

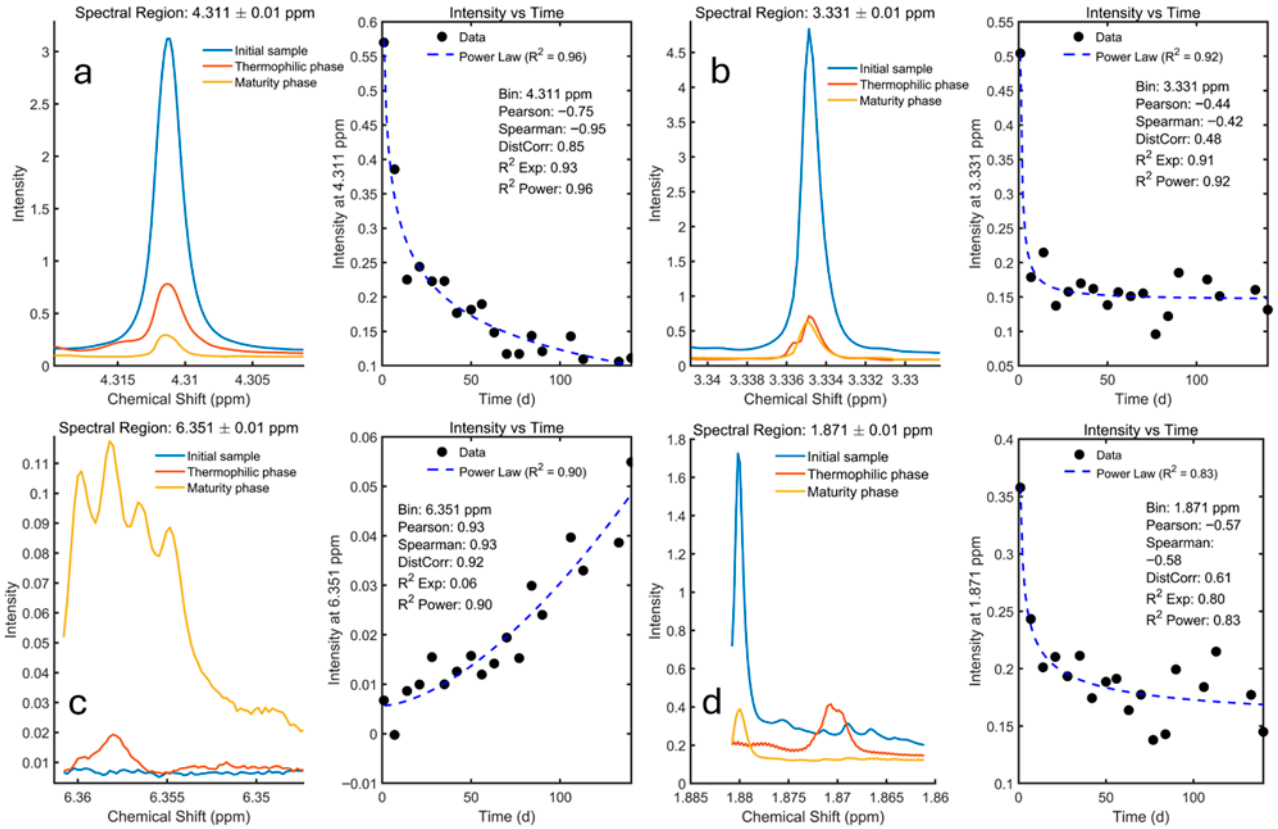


Figure 5. Representative windows for the highest-scoring bins, illustrating signal trajectories and fitted models: (**a**) tartrate at $\delta \approx 4.323$ ppm (R^2_power ≈ 0.96), (**b**) methanol at $\delta \approx 3.347$ ppm ($R^2 \approx 0.92$, declining), (**c**) aromatic feature at $\delta \approx 6.351$ ppm (tentative assignment; $R^2 \approx 0.90$), and (**d**) thymidine at $\delta \approx 1.851$ ppm ($R^2 \approx 0.83$).

Specifically, we evaluated Pearson (linear) and Spearman (rank/monotonic) coefficients together with power and exponential fits (reporting R^2), selecting intervals that maximized association irrespective of sign (negative for disappearing signals; positive for growing signals). The algorithm then ranked bins by consensus across metrics, and we visually verified the trajectories, retaining only those consistent with chemically interpretable assignments. Notably, the tartrate region ($\delta \approx 4.323$ ppm) showed the strongest relationship ($R^2 \approx 0.96$), followed by methanol ($\delta \approx 3.347$ ppm; $R^2 \approx 0.92$, declining), and thymidine ($\delta \approx 1.851$ ppm; $R^2 \approx 0.83$). An aromatic feature at $\delta \approx 6.351$ ppm increased with time ($R^2 \approx 0.90$); while its assignment remains tentative (acrylamide), its robust fit and agreement across metrics argue for genuine time dependence. Together, these correlations mirror the overall trajectory observed elsewhere in the spectra—rapid depletion of labile pools and progressive aromatic enrichment—showing that ^{1}H NMR coupled to chemometrics yields compact, mechanistically credible maturity markers beyond traditional physicochemical indicators.

Although the overall molecular trajectory of the WEOM—characterized by the rapid depletion of amino acids and carbohydrates, the transient accumulation of organic acids, and the gradual enrichment in aromatic structures—is comparable to that reported in other composting studies, specific differences arise from the composition of the feedstock and the process conditions. The poultry-manure fraction, rich in nitrogen and proteins, enhances amino acid turnover and the production of short-chain acids, whereas the winery residues contribute tartrate, glycerol, and phenolic compounds that yield distinctive spectral features in the aromatic and carboxylic regions. In addition, the controlled aeration of the Rutgers system maintained thermophilic and oxic conditions, favoring oxidative stabilization over fermentative pathways and minimizing alcohol accumulation. Similar substrate- and aeration-dependent variations have been described by [22,44]. These differences underline the flexibility of the NMR–chemometric approach for capturing both common and system-specific molecular patterns during composting.

However, the method requires access to high-resolution NMR instrumentation and computational expertise. Additionally, the structural assignment of specific compounds remains a challenge in highly complex matrices, which may limit the mechanistic interpretation of spectral changes.

4. Discussion

4.1. Molecular Trajectory of WEOM During Composting

The ^{1}H NMR data reveal a consistent biochemical trajectory of the water-extractable organic matter (WEOM): rapid loss of labile, hydrophilic solutes (amino acids, simple sugars, and volatile fatty acids, VFAs) followed by progressive enrichment of aromatic features that mark humification. This pattern aligns with earlier NMR descriptions of compost maturation, where O-alkyl signatures decline and aromatic/phenolic resonances intensify as compost stabilizes [1–3]. In our system, the transient accumulation of VFAs—dominated by acetate (~285‰; 1.91 ppm)—and the prominence of lactate (~60‰; 1.32 ppm) and formate (~49‰; 8.44 ppm) during early stages fit well with acidogenic metabolism reported for manure-rich mixtures [4–6].

4.2. Rapid Turnover of Amino Acids and Sugars, and Consequences for Process Control

Amino acids (valine, leucine, isoleucine, glutamate) decreased swiftly, reflecting preferential microbial uptake of N-bearing solutes; their fast depletion agrees with ^{1}H/^{13}C-NMR reports on WEOM dynamics during composting [2,3,9]. From an operational standpoint, such early-stage markers can serve as sentinel signals for transition out of the mesophilic phase [12,13]. Their systematic monitoring—together with VFAs—offers a practical way to detect suboptimal aeration or excessive acidogenesis that might delay stabilization [4–6].

4.3. Winery-Specific Molecular Fingerprints and Their Mechanistic Basis

Several constituents reinforce the vinicultural imprint of the feedstock. Glycerol (≈9.8‰; 3.77 ppm) and tartrate were consistently detected, as expected for grape-derived residues; both are canonical markers of winery by-products [9–11]. Notably, glycerol fluctuations—with phases of decline followed by reappearance—are mechanistically plausible: delayed enzymatic hydrolysis of lipid-rich matrices (yeast remnants, residual fats) can release glycerol later in the process, and localized micro-anaerobic niches may support transient glycerol production or accumulation by microbes [4]. In addition, the suite of dicarboxylic acids included suberate (octanedioate) (>110‰ total), which we attribute to a combination of ω-oxidation of fatty acids and suberin inputs (cork). Migration of suberin-derived monomers (including suberic acid) from cork to hydroalcoholic media/wines has been documented, supporting this matrix-specific source [11–13].

4.4. Minor Constituents That Inform on Pathway Chemistry

Low-abundance features provided diagnostic insight into pathway chemistry often overlooked by bulk indicators. In the 0–5 ppm window, a persistent levulinate triplet (~2.74–2.75 ppm) points to carbohydrate dehydration/rearrangement chemistry occurring in acidic microenvironments—chemistry that can be sustained even as other labile pools wane [23]. We also observed signals consistent with choline catabolism products (e.g., TMA/TMAO, N,N-dimethylglycine/sarcosine) that suggest operation of the CutC pathway in acidogenic/anaerobic niches, and traces of 3-/4-hydroxybutyrate compatible with storage-polymer turnover [39,50,52]. In the 5–10 ppm region, syringic and p-hydroxybenzoic acids support a grape-phenolic fingerprint, while xanthine/hypoxanthine and uracil reflect nucleic-acid turnover in microbial biomass and contributions from poultry litter [31,47]. A specific aromatic feature at 6.351 ppm exhibited a strong monotonic increase with time ($R^2 \approx 0.90$) and was tentatively associated with acrylamide on chemical-shift grounds; this assignment should remain tentative pending targeted MS confirmation, yet its consistent time trend suggests a useful empirical maturity marker in our dataset [6]. Future work should validate tentative assignments and minor markers with MS.

4.5. From Qualitative Fingerprints to Quantitative Prediction

Beyond descriptive trends, the biPLS model built on binned spectra provided strong time-prediction performance (r = 0.951; RMSECV = 13.04 days over 212 days, ≈6.2% relative error) [19,54,58]. Informative intervals (0.8–1.5, 2.6–2.9, 3.9–4.2, and 5.0–5.7 ppm) coincide with chemically interpretable domains (aliphatic amino-acid region; VFA/ketone region; carbohydrates/alcohols; olefinic/anomeric), and include features such as lactate (1.33; 4.10–4.12 ppm), suberate (~1.29–1.32 ppm), and levulinate (~2.74–2.75 ppm) identified in univariate trajectories [9]. These convergences between univariate markers and multivariate selection enhance confidence in the model's mechanistic plausibility. At the same time, careful safeguards against overfitting are essential: cross-validation and backward interval pruning are necessary but should be complemented by independent test sets in future applications to fully certify generalization performance in operational settings [18].

4.6. Practical Implications for Compost Monitoring and Quality Assurance

The combination of full-spectrum ^{1}H NMR and focused chemometrics offers a dual utility [22]. First, it yields a mechanistic fingerprint of compost evolution—sensitive to shifts in labile pools, emergence of aromaticity, and matrix-specific markers (e.g., tartrate, glycerol, suberate). Second, it enables quantitative time-tracking, which could support real-time or near-real-time decisions on aeration, turning, or moisture management. The strong correlations observed for tartrate ($R^2 \approx 0.96$, power), methanol ($R^2 \approx 0.92$), and the 6.351 ppm feature ($R^2 \approx 0.90$) illustrate how a small panel of NMR variables might be used as a lean maturity index when resources preclude full multivariate modeling [6,12].

4.7. Limitations and Avenues for Further Research

Two limitations merit discussion. First, compound assignment in complex matrices is inherently challenging. While many identifications are robust and supported by literature, some mechanistic interpretations—such as those involving intermediate pathways of oxidation, dehydration, or aromatic condensation—are hypothesis-driven rather than experimentally verified. These biochemical trends are consistent with previous composting and soil organic matter studies [2,6,47], but do not constitute direct mechanistic proof. In particular, minor signals such as the aromatic feature at 6.351 ppm were interpreted based on reproducible time-dependent behavior and plausible chemical shift domains, yet they remain tentative and require orthogonal confirmation. To strengthen confidence in these

molecular assignments, targeted LC–MS/MS and multidimensional NMR analyses (COSY, HSQC, HMBC) should be conducted in future studies. Additionally, the use of controlled biodegradation assays and isotopic labeling experiments is planned to experimentally validate the proposed transformation pathways and clarify the biochemical origin of diagnostic spectral features.

Second, instrumentation and expertise can be barriers to adoption; however, targeted spectral panels and simplified workflows could lower the entry threshold for routine monitoring. Despite the analytical power of high-field ^{1}H NMR spectroscopy, its application in routine compost monitoring remains limited by the need for costly instrumentation and specialized expertise. Recent advances in benchtop or low-field NMR (40–80 MHz) technology allow the acquisition of relaxation-based and bulk-proton mobility parameters that correlate with compost maturity, requiring minimal sample handling [60,61]. Short aqueous extraction protocols ($\leq$1 h) and direct measurement of the water-soluble fraction can further simplify the procedure and enhance throughput. Moreover, the diagnostic intervals identified by the biPLS model (1.27–1.38, 2.53–2.76, 4.02–4.13 ppm) could be exploited to develop simplified spectral indices for semi-quantitative evaluation of compost stability. In this framework, high-field NMR would serve as a reference tool for model calibration, while compact NMR instruments or complementary spectroscopic techniques (fluorescence EEM, FTIR) could act as rapid, cost-efficient surrogates for large-scale compost quality assurance [2,6]. Future work should therefore (i) validate tentative assignments and minor markers with MS and multidimensional NMR, (ii) test model transferability across other waste mixtures and operational conditions, (iii) integrate independent test sets and external validation for biPLS pipelines, and (iv) link NMR markers with soil response after field application to strengthen the agronomic relevance of molecular maturity indicators.

5. Conclusions

This study demonstrates that ^{1}H NMR spectroscopy of the water-extractable organic matter (WEOM), combined with interval-based chemometric modeling, provides a robust molecular-level framework for assessing composting dynamics. The spectral evolution revealed a rapid depletion of amino acids and carbohydrates, the transient accumulation of low-molecular-weight organic acids, and the gradual enrichment of aromatic and phenolic structures associated with humification.

The integration of iPLS and biPLS regression models enabled accurate prediction of composting time ($r \approx 0.95$) and identification of diagnostic spectral regions linked to key metabolites. These findings confirm the high sensitivity of NMR-based chemometric tools to capture both biochemical and structural transformations during composting.

Beyond analytical insight, this approach offers a promising strategy for real-time monitoring and quality control in compost production. High-field NMR can serve as a reference platform for calibration, while simplified spectral indices or low-field instruments could translate these advances into practical tools for industrial-scale compost management.

Future work will focus on validating these molecular indicators across different waste mixtures and operational conditions, paving the way toward a standardized, spectroscopic methodology for compost stability and maturity assessment.

Author Contributions: Funding obtained: F.C.M.-E., R.M. and M.P. Conceived and designed the experiments: R.G.-Á., M.P., M.Á.B. and F.C.M.-E. Performed the analysis and figures: R.G.-Á. and F.C.M.-E. Analyzed the data: R.G.-Á., E.M.-S., J.A.S.-T., L.O., C.P., M.P. and F.C.M.-E. Wrote the manuscript: R.G.-Á. and F.C.M.-E. Reviewed the manuscript: R.G.-Á., E.M.-S., M.Á.B., J.A.S.-T., L.O., C.P., M.P., R.M. and F.C.M.-E. All authors have read and agreed to the published version of the manuscript.

Funding: This research received no external funding.

Institutional Review Board Statement: Not applicable.

Informed Consent Statement: Not applicable.

Data Availability Statement: The data presented in this study are available on request from the corresponding author.

Conflicts of Interest: The authors declare no conflicts of interest.

References

1. Moreno-Casco, J.; Moral-Herrero, R. *Compostaje*; Ediciones Mundi-Prensa: Madrid, Spain, 2008.
2. Marhuenda-Egea, F.C.; Martinez-Sabater, E.; Jorda, J.; Moral, R.; Bustamante, M.A.; Paredes, C.; Perez-Murcia, M.D. Dissolved organic matter fractions formed during composting of winery and distillery residues: Evaluation of the process by fluorescence excitation-emission matrix. *Chemosphere* **2007**, *68*, 301–309. [CrossRef] [PubMed]
3. Dell'Abate, M.T.; Benedetti, A.; Sequi, P. Thermal methods of organic matter maturation monitoring during a composting process. *J. Therm. Anal. Calorim.* **2000**, *61*, 389–396. [CrossRef]
4. Bertrán, E.; Sort, X.; Soliva, M.; Trillas, I. Composting winery waste: Sludge and grape stalks. *Bioresour. Technol.* **2004**, *95*, 203–208. [CrossRef]
5. Provenzano, M.R.; de Oliveira, S.C.; da Silva, M.R.; Senesi, N. Assessment of maturity degree of composts from domestic solid wastes by fluorescence and Fourier transform infrared spectroscopies. *J. Agric. Food Chem.* **2001**, *49*, 5874–5879. [CrossRef]
6. Provenzano, M.R.; Malerba, A.D.; Pezzolla, D.; Gigliotti, G. Chemical and spectroscopic characterization of organic matter during the anaerobic digestion and successive composting of pig slurry. *Waste Manag.* **2014**, *34*, 653–660. [CrossRef]
7. Bustamante, M.A.; Moral, R.; Paredes, C.; Vargas-García, M.C.; Suárez-Estrella, F.; Moreno, J. Evolution of the pathogen content during co-composting of winery and distillery wastes. *Bioresour. Technol.* **2008**, *99*, 7299–7306. [CrossRef]
8. Youness, B.; Lyamlouli, K.; Oudouch, Y.; El Boukhari Mohamed, E.M.; Hafidi, M. Agronomic assessment of solar dried recycled olive mill sludge on Maize agrophysiological traits and soil fertility. *Int. J. Recycl. Org. Waste Agric.* **2022**, *11*, 247–261. [CrossRef]
9. Bustamante, M.A.; Paredes, C.; Marhuenda-Egea, F.C.; Pérez-Espinosa, A.; Bernal, M.P.; Moral, R. Co-composting of distillery wastes with animal manures: Carbon and nitrogen transformations in the evaluation of compost stability. *Chemosphere* **2008**, *72*, 551–557. [CrossRef]
10. Chen, Y.; Inbar, Y. Chemical and spectroscopical analyses of organic matter transformations during composting in relation to compost maturity. In *Science and Engineering of Composting: Design, Environmental, Microbiological and Utilization Aspects*; Hoitink, H.A.J., Keener, H.M., Eds.; Renaissance Publications: Worthington, OH, USA, 1993; pp. 551–600.
11. Haug, R.T. *The Practical Handbook of Compost Engineering*; CRC Press: Boca Raton, FL, USA, 1993.
12. Goyal, S.; Dhull, S.K.; Kapoor, K.K. Chemical and biological changes during composting of different organic wastes and assessment of compost maturity. *Bioresour. Technol.* **2005**, *96*, 1584–1591. [CrossRef]
13. Bernal, M.P.; Alburquerque, J.A.; Moral, R. Composting of animal manures and chemical criteria for compost maturity assessment: A review. *Bioresour. Technol.* **2009**, *100*, 5444–5453. [CrossRef] [PubMed]
14. Khan, M.M.; Siddiqi, S.A.; Farooque, A.A.; Iqbal, Q.; Shahid, S.A.; Akram, M.T.; Rahman, S.; Al-Busaidi, W.; Khan, I. Towards Sustainable Application of Wastewater in Agriculture: A Review on Reusability and Risk Assessment. *Agronomy* **2022**, *12*, 1397. [CrossRef]
15. Chikae, M.; Ikeda, R.; Kerman, K.; Morita, Y.; Tamiya, E. Estimation of maturity of compost from food wastes and agro-residues by multiple regression analysis. *Bioresour. Technol.* **2006**, *97*, 1979–1985. [CrossRef]
16. Simpson, A.J. Determining the molecular weight, aggregation, structures and interactions of natural organic matter using diffusion ordered spectroscopy. *Magn. Reson. Chem.* **2002**, *40*, S72–S82. [CrossRef]
17. Levitt, M.H. *Spin Dynamics: Basics of Nuclear Magnetic Resonance*; John Wiley & Sons: Chichester, UK, 2001.
18. Preston, C.M. Applications of NMR to soil organic matter analysis: History and prospects. *Soil Sci.* **1996**, *161*, 144–166. [CrossRef]
19. Norgaard, L.; Saudland, A.; Wagner, J.; Nielsen, J.P.; Munck, L.; Engelsen, S.B. Interval Partial Least-Squares Regression (iPLS): A Comparative Chemometric Study with an Example from Near-Infrared Spectroscopy. *Appl. Spectrosc.* **2000**, *54*, 413–419. Available online: https://opg.optica.org/as/abstract.cfm?URI=as-54-3-413 (accessed on 24 November 2025). [CrossRef]
20. Winning, H.; Viereck, N.; Nørgaard, L.; Larsen, K.L.; Engelsen, S.B. Quantification of the degree of blockiness in pectins using 1H NMR spectroscopy and chemometrics. *Carbohydr. Res.* **2007**, *342*, 1261–1272. [CrossRef]
21. Finstein, M.S.; Miller, F.C.; MacGregor, S.T.; Psarianos, K.M. *The Rutgers Strategy for Composting: Process Design and Control*; U.S. EPA Water Engineering Research Laboratory: Cincinnati, OH, USA, 1985.

22. Torres-Climent, A.; Gomis, P.; Martin-Mata, J.; Bustamante, M.A.; Marhuenda-Egea, F.C.; Perez-Murcia, M.D.; Perez-Espinosa, A.; Paredes, C.; Moral, R. Chemical, Thermal and Spectroscopic Methods to Assess Biodegradation of Winery-Distillery Wastes during Composting. *PLoS ONE* **2015**, *10*, e0138925. [CrossRef]
23. Kögel-Knabner, I. Analytical approaches for characterizing soil organic matter. *Org. Geochem.* **2000**, *31*, 609–625. [CrossRef]
24. Lynd, L.R.; Weimer, P.J.; van Zyl, W.H.; Pretorius, I.S. Microbial cellulose utilization: Fundamentals and biotechnology. *Microbiol. Mol. Biol. Rev.* **2002**, *66*, 506–577. [CrossRef] [PubMed]
25. Chalbot, M.C.; Siddiqui, S.; Kavouras, I.G. Molecular Speciation of Size Fractionated Particulate Water-Soluble Organic Carbon by Two-Dimensional Nuclear Magnetic Resonance (NMR) Spectroscopy. *Int. J. Environ. Res. Public Health* **2021**, *18*, 1334. [CrossRef] [PubMed]
26. Zhao, Y.; Ma, C.; Cai, R.; Xin, L.; Li, Y.; Ke, L.; Ye, W.; Ouyang, T.; Liang, J.; Wu, R.; et al. NMR and MS reveal characteristic metabolome atlas and optimize esophageal squamous cell carcinoma early detection. *Nat. Commun.* **2024**, *15*, 2463. [CrossRef] [PubMed]
27. Wagner, L.; Gomez-Requeni, P.; Moazzami, A.A.; Lundh, T.; Vidakovic, A.; Langeland, M.; Kiessling, A.; Pickova, J. 1H NMR-based metabolomics and lipid analyses revealed the effect of dietary replacement of microbial extracts or mussel meal with fish meal to arctic charr (*Salvelinus alpinus*). *Fishes* **2019**, *4*, 46. [CrossRef]
28. Paul, J.W.; Beauchamp, E.G. Short-term effects of nitrogen fertilizers, liming, and straw on volatile fatty acid production in poultry manure. *Biol. Fertil. Soils* **1989**, *8*, 20–24. [CrossRef]
29. Yin, J.; Wang, K.; Chen, C. Volatile fatty acids recovery from poultry manure: A review. *J. Environ. Manag.* **2022**, *303*, 114240. [CrossRef]
30. Said-Pullicino, D.; Erriquens, F.G.; Gigliotti, G. Changes in the water extractable organic matter during composting of municipal solid wastes. *Waste Manag.* **2007**, *27*, 1730–1740. [CrossRef]
31. Caricasole, P.; Provenzano, M.R.; Hatcher, P.G.; Senesi, N.; Brunetti, G. Composting of municipal solid wastes: Characterization of organic matter by CPMAS 13C NMR spectroscopy. *Bioresour. Technol.* **2010**, *101*, 823–829. [CrossRef]
32. He, X.T.; Logan, T.J.; Traina, S.J. Physical and chemical characteristics of water extractable organic matter from composts. *Chemosphere* **2011**, *82*, 541–547. [CrossRef]
33. Jan, M.T.; Roberts, P.; Tonheim, S.K.; Jones, D.L. Protein breakdown represents a major bottleneck in nitrogen cycling in grassland soils. *Soil Biol. Biochem.* **2009**, *41*, 2272–2282. [CrossRef]
34. Torres, N.; Tobón-Cornejo, S.; Velazquez-Villegas, L.A.; Noriega, L.G.; Alemán-Escondrillas, G.; Tovar, A.R. Amino Acid Catabolism: An Overlooked Area of Metabolism. *Nutrients* **2023**, *15*, 3378. [CrossRef]
35. Zhai, W.; Li, X.; Duan, X.; Gou, C.; Wang, L.; Gao, Y. Development of a microbial protease for composting swine carcasses, optimization of its production and elucidation of its catalytic hydrolysis mechanism. *BMC Biotechnol.* **2022**, *22*, 36. [CrossRef]
36. El Fels, L.; Naylo, A.; Jemo, M.; Zrikam, N.; Boularbah, A.; Ouhdouch, Y.; Hafidi, M. Microbial enzymatic indices for predicting composting quality of recalcitrant lignocellulosic substrates. *Front. Microbiol.* **2024**, *15*, 1423728. Available online: https://www.frontiersin.org/journals/microbiology/articles/10.3389/fmicb.2024.1423728 (accessed on 24 November 2025). [CrossRef]
37. Vranova, V.; Zahradnickova, H.; Janous, D.; Skene, K.R.; Matharu, A.S.; Rejsek, K.; Formanek, P. The significance of D-amino acids in soil, fate and utilization by microbes and plants: Review and identification of knowledge gaps. *Plant Soil* **2012**, *354*, 21–39. [CrossRef]
38. Akita, H.; Fujino, Y.; Doi, K.; Ohshima, T. Highly stable meso-diaminopimelate dehydrogenase from an Ureibacillus thermosphaericus strain A1 isolated from a Japanese compost: Purification, characterization and sequencing. *AMB Express* **2011**, *1*, 43. [CrossRef] [PubMed]
39. Le Mao, I.; Valls Fonayet, J.; Wirth, J. NMR-based metabolomics applied to wine quality analysis. *Food Chem.* **2021**, *350*, 129263. [CrossRef]
40. Wilkes, E. Typical values for fats, proteins and salt in Australian wine for nutritional labelling. *AWRI Tech. Rev.* **2023**, *No. 266*. Available online: https://www.awri.com.au/information_services/technical_review/technical-notes/technical-note-typical-values-for-fats-proteins-and-salt-in-australian-wine-for-nutritional-labelling/ (accessed on 24 November 2025).
41. Zacharof, M.P. Grape winery waste as feedstock for bioconversion: Applying the biorefinery concept. *Waste Biomass Valorization* **2017**, *8*, 1011–1025. [CrossRef]
42. Graça, J.; Pereira, H. Methanolysis of bark suberins: Analysis of glycerol and acid monomers. *Phytochem. Anal.* **2000**, *11*, 45–51. [CrossRef]
43. Cordeiro, N.; Belgacem, M.N.; Silvestre, A.J.D.; Neto, C.P.; Gandini, A. Cork suberin as a new source of chemicals. *Int. J. Biol. Macromol.* **1998**, *22*, 71–80. [CrossRef]
44. Caricasole, P.; Provenzano, M.R.; Hatcher, P.G.; Senesi, N. Chemical characteristics of dissolved organic matter during composting of different organic wastes assessed by 13C CPMAS NMR spectroscopy. *Bioresour. Technol.* **2010**, *101*, 8232–8236. [CrossRef]

45. Yu, Z.; Liu, X.; Zhao, M.; Zhao, W.; Liu, J.; Tang, J.; Liao, H.; Chen, Z.; Zhou, S. Hyperthermophilic composting accelerates the humification process of sewage sludge: Molecular characterization of dissolved organic matter using EEM–PARAFAC and two-dimensional correlation spectroscopy. *Bioresour. Technol.* **2019**, *274*, 198–206. [CrossRef]
46. Silva, A.C.; Rocha, P.; Valderrama, P.; Antelo, J.; Geraldo, D.; Proença, M.F.; Fiol, S.; Bento, F. A Correlation-Based Approach for Predicting Humic Substance Bioactivity from Direct Compost Characterization. *Molecules* **2025**, *30*, 1511. [CrossRef] [PubMed]
47. Fuentes, M.; Baigorri, R.; González-Gaitano, G.; García-Mina, J.M. The complementary use of 1H NMR, 13C NMR, FTIR and size exclusion chromatography to investigate the principal structural changes associated with composting of organic materials with diverse origin. *Org. Geochem.* **2007**, *38*, 2012–2023. [CrossRef]
48. International Organisation of Vine and Wine. *International Code of Oenological Practices*; Organisation Internationale de la Vigne et du Vin: Dijon, France, 2023.
49. Le, T.-K.; Lee, Y.-J.; Han, G.H.; Yeom, S.-J. Methanol Dehydrogenases as a Key Biocatalysts for Synthetic Methylotrophy. *Front. Bioeng. Biotechnol.* **2021**, *9*, 787791. Available online: https://www.frontiersin.org/journals/bioengineering-and-biotechnology/articles/10.3389/fbioe.2021.787791 (accessed on 24 November 2025). [CrossRef]
50. Vu Huong, N.; Subuyuj Gabriel, A.; Vijayakumar, S.; Good Nathan, M.; Martinez-Gomez, N.C.; Skovran, E. Lanthanide-Dependent Regulation of Methanol Oxidation Systems in Methylobacterium extorquens AM1 and Their Contribution to Methanol Growth. *J. Bacteriol.* **2016**, *198*, 1250–1259. [CrossRef]
51. Keppler, F.; Hamilton, J.T.G.; McRoberts, W.C.; Vigano, I.; Braß, M.; Röckmann, T. Methoxyl groups of plant pectin as a precursor of atmospheric methane: Evidence from deuterium labelling studies. *New Phytol.* **2008**, *178*, 808–814. [CrossRef]
52. Macey, M.C.; Pratscher, J.; Crombie, A.T.; Murrell, J.C. Impact of plants on the diversity and activity of methylotrophs in soil. *Microbiome* **2020**, *8*, 31. [CrossRef]
53. Sánchez-Monedero, M.A.; Fernández-Hernández, A.; Higashikawa, F.S.; Cayuela, M.L. Relationships between emitted volatile organic compounds and their concentration in the pile during municipal solid waste composting. *Waste Manag.* **2018**, *79*, 179–187. [CrossRef]
54. Leardi, R.; Nørgaard, L. Sequential application of backward interval partial least squares and genetic algorithms for the selection of relevant spectral regions. *J. Chemom.* **2004**, *18*, 486–497. [CrossRef]
55. Martínez-Sabater, E.; Bustamante, M.A.; Marhuenda-Egea, F.C.; El-Khattabi, M.; Moral, R.; Lorenzo, E.; Paredes, C.; Gálvez, L.N.; Jordá, J.D. Study of the evolution of organic matter during composting of winery and distillery residues by classical and chemometric analysis. *J. Agric. Food Chem.* **2009**, *57*, 9613–9623. [CrossRef]
56. Cáceres, R.; Coromina, N.; Marfà, O. Composting of greenhouse tomato plant residues: Maturity assessment and agronomic value. *Waste Manag.* **2018**, *79*, 141–152. [CrossRef]
57. Ståhle, L.; Wold, S. Partial least squares analysis with cross-validation for the two-class problem: A Monte Carlo study. *J. Chemom.* **1987**, *1*, 185–196. [CrossRef]
58. Esbensen, K.H.; Geladi, P. Principles of Proper Validation: Use and abuse of re-sampling for validation. *J. Chemom.* **2010**, *24*, 168–187. [CrossRef]
59. Trygg, J.; Wold, S. Orthogonal projections to latent structures (O-PLS). *J. Chemom.* **2002**, *16*, 119–128. [CrossRef]
60. Dufour-Rainfray, D.; Lambérioux, M.; Boulard, P.; Guidotti, M.; Delaye, J.; Ribeiro, M.; Gauchez, A.; Balageas, A.; Emond, P.; Agin, A. Metabolomics—An overview. From basic principles to potential biomarkers (part 2). *Med. Nucl.-Imag. Fonct. Metab.* **2020**, *44*, 158–163. [CrossRef]
61. Blümich, B. Low-field and benchtop NMR. *J. Magn. Reson.* **2019**, *306*, 27–35. [CrossRef]

Disclaimer/Publisher's Note: The statements, opinions and data contained in all publications are solely those of the individual author(s) and contributor(s) and not of MDPI and/or the editor(s). MDPI and/or the editor(s) disclaim responsibility for any injury to people or property resulting from any ideas, methods, instructions or products referred to in the content.